Impacts of application patterns and incorporation rates of dredged Yellow River sediment on structure and infiltration of saline-alkali soil

Kesheng Li[1,2], Weihang Kong[2], Wenshuo Xu[2], Chuanxiao Liu[2*]

(1. *State Key Laboratory for Geomechanics and Deep Underground Engineering, China University of Mining and Technology, Xuzhou 221116, Jiangsu, China*;

2. *College of Water Conservancy and Civil Engineering, Shandong Agricultural University, Tai'an 271018, Shandong, China*)

Abstract: Soil salinization is an issue of global concern. Despite recent evidence indicates that application of sediments into saline-alkali soil in Yellow River Delta as an additive can increase crop yield, its effects on soil structure and infiltration remain uncertain. In this study, the comprehensively analyses were conducted on the soil infiltration and microstructure of the soil treated with three sediment application layers (surface layer at 0-15 cm, lower layer at 15-30 cm, and plough layer at 0-30 cm) and four sediment incorporation rates (0, 2%, 5% and 10%), using soil column simulation experiment. Results indicated that the dredged Yellow River sediments can improve the infiltration capacity of saline-alkali soil; and the infiltration capacity increased with the rising sediment incorporation rate under the given application pattern. Compared with the control, applying dredged Yellow River sediments at 10% rate at lower layer and plough layer significantly facilitated the soil infiltration of the saline-alkali soil. Soil macro-porosity for T2, T5 and T10 was 26%, 52% and 158% more than that for the control, respectively. This phenomenon was attributed to the increased soil macro-porosity, due to the improved soil microstructure with the incorporation of sediment into the saline-alkali soil. Moreover, the cumulative infiltration was fitted better with Kostiakov infiltration model than Horton and Philip models.

Keywords: saline-alkali soil, Yellow River sediment, soil infiltration, microstructure, incorporation rate, application pattern

DOI: 10.25165/j.ijabe.20221504.6556

Citation: Li K S, Kong W H, Xu W S, Liu C X. Impacts of application patterns and incorporation rates of dredged Yellow River sediment on structure and infiltration of saline-alkali soil. Int J Agric & Biol Eng, 2022; 15(4): 139–146.

1 Introduction

Soil salinization is one of the major problems in global agriculture because it can lead to soil degradation and undermine the productivity of cultivated land[1,2]. The global saline-alkali land area accounts for about 10% of the total land area[3], while the wasteland caused by salinization is about 34.6 million hm^2 in China[4]. Typical physical features for saline-alkali soil include non-ventilation and poor water permeability, which severely restricts the ecological reservation as well as economic and social development[5,6]. Due to the shortage of irrigation water, shallow level, and groundwater salinization, soil salinization is becoming an increasingly severe challenge in coastal areas.

Currently, studies on the remediation of saline-alkali soil mainly focus on two aspects, namely, cutting off the rising capillarity, and improving the physical properties of these soils' degradation. Previous studies mainly adopted different particle sizes, thickness and materials to achieve the barrier design to cut off capillarity[7-10]. Although this measure effectively blocked the rise of groundwater, there are also reports on the failures of these barriers in reducing salinization[11,12]. Given the compact structure and poor permeability of saline-alkali soil, other remediation techniques need to be implemented prior to restricting the salinity source. Base on this idea, a series of measures have been practiced to improve soil properties according to specific site conditions, such as improved tillage methods[13,14], incorporation of plant residues[15,16], the application of zeolite[17], chemical remediation[18-20] and organic amendments[21]. The application of biochar and flue-gas desulphurization (FGD) gypsum is considered to be the most effective measure[22,23], but it is not widely used because of its high cost and its tendency to cause food safety problems, especially in developing countries. Until now, few studies have considered restoring saline soils by improving soil texture; and in this regard, sediment has been considered to be an effective additive[24,25], because it can fundamentally remedy the undesirable properties of these soils. Besides, reasonable application of sediment, which is typically considered as wastes, is environmentally friendly. Despite these advantages, whether sediment addition can change soil infiltration remains uncertain.

In the 1920s, Terzaghi, father of soil mechanics, proposed that the microstructural characteristics of soil should be considered when studying its properties. Previous research generally indicates that both the physical and mechanical properties of soil depend on its microstructure[26-30]. Fei et al.[31] investigated the influences of the straw biochar and anionic PAM on soil structure and found that high proportion of biochar significantly improves soil porosity. Wei et al.[32] qualitatively and quantitatively characterized the microstructure and parameters of loess in 3D space using scanning electron microscope (SEM) and CT technology. Wang et al.[33] explored the evolution of the microstructure and pore size distribution caused by consolidation in

Received date: 2021-02-28 **Accepted date:** 2022-05-05

Biographies: **Kesheng Li**, PhD candidate, research interests: geotechnical engineering and soil remediation, Email: 2018110553@sdau.edu.cn; **Weihang Kong**, Master, research interests: agricultural water-soil engineering, Email:2019120640@sdau.edu.cn; **Wenshuo Xu**, Master candidate, research interests: frozen soil engineering and soil remediation, Email: 2019110564@sdau.edu.cn.

***Corresponding author: Chuanxiao Liu**, PhD, Professor, research interests: geotechnical engineering and soil remediation. College of Water Conservancy and Civil Engineering, Shandong Agricultural University, Tai'an 271018, China. Tel: +86-538-8241865, Email: lchuanx@163.com.

both intact and remolded loess. Li et al.[34] interpreted the microstructural evolution of loess soils arising from loading and wetting using SEM. However, the research on soil microstructure in China has mainly focused on collapsible loess, and current research on the microstructure of saline-alkali soil is inadequate. Recent studies using X-ray micro-CT have shown that a higher proportion of biochar can be used to improve the porosity of saline alkali soil[31]. Additionally, our recent study indicated that the permeability of undisturbed saline-alkali soil in the Yellow River Delta was determined by its microstructure[35-37]. Mao et al.[24,25] reported for the first time that the applying dredged sediment improved soil salinity environment and the yield of cotton and wheat. However, at present, the research on the dredged Yellow River sediment mainly focuses on its effect on the chemical properties and saturated hydraulic conductivity of saline soil, and the research on the effects of sediment application methods and incorporation rates on soil water infiltration and microstructure is relatively limited.

This study focused on whether the application of dredging the Yellow River sediment can improve the microstructure of saline-alkali soil, so as to improve its permeability characteristics. The objectives of this study were to: (i) compare the soil infiltration of saline-alkali soils under different sediment incorporation rates and application patterns, (ii) quantify the microstructural characteristics of saline-alkali soils with different sediment incorporation rates, (iii) evaluate the applicabiliyies of commonly-used infiltration models such as Kostiakov's, Philip's and Horton's models.

2 Materials and methods

2.1 Experimental materials

The experimental soil was taken from a flat wasteland near Binhai New District (37°17′41″N, 118°45′37″E), Dongying City, Shandong Province, China (Figure 1). In order to reduce the error, Z-shaped soil sampling method was used to obtain disturbed soil at a depth of 0-20 cm. After the soil was air dried naturally, it was passed through a 2 mm soil sieve to remove impurities, and mixed well for spare. In addition, undisturbed soil was taken from the site, and the average soil bulk density was measured to be 1.46 g/cm^3. The soil electric conductivity was measured to be 12.44 dS/m with a conductivity meter, proving it was heavy saline-alkali soil. The basic physicochemical properties of the soil are listed in Table 1.

The sediment used for the test was local dredged Yellow River sediment, which was sifted with a 2 mm sieve. After removing impurities, the dredged sediment was washed and dried for spare. The dredged sediment contained 0.96% clay (<0.002 mm), 3.55% silt (0.002-0.02 mm), and 95.49% sand (>0.02 mm).

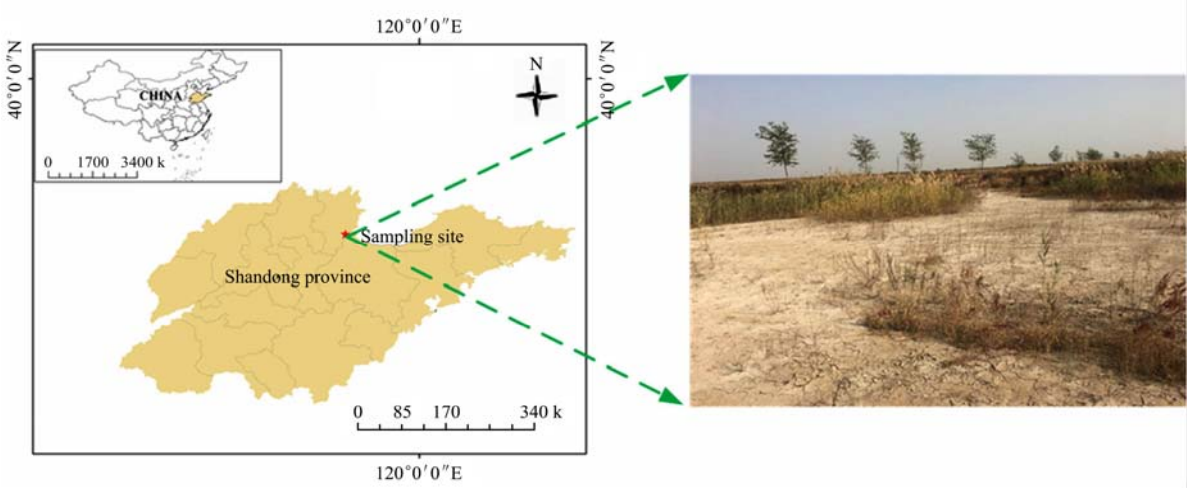

Figure 1 Location map of the Yellow River Delta and the sampling site

Table 1 Characteristics of the local saline-alkali soil

Source of variation		Saline-alkali soil
pH[a]		8.78 (0.05)
Bulk density/g·cm^{-3}		1.46 (0.11)
Electrical conductivity[a]/dS·m^{-1}		12.44 (0.25)
Soluble salt/g·kg^{-1}		34.09 (0.08)
Cation exchange capacity/cmol·kg^{-1}		20.58 (0.05)
Sodium adsorption ratio/(mmol·L^{-1})$^{1/2}$		312.7 (0.20)
Saturated hydraulic conductivity/cm·s^{-1}		3.58×10^{-5}
Clay (< 0.002 mm)		8.24 (0.05)
Silt (0.02-0.002 mm)		38.20 (0.12)
Sand (0.02-2 mm)	0.2-0.02 mm	53.54 (0.15)
	2-0.2 mm	0.02 (0.01)

Note: [a] Soil EC and pH were measured using 1:5 mixture of soil and water. Values in parenthesis are standard error.

The soil minerals were qualitatively and quantitatively analyzed using a TD-3500 X-ray diffractometer (Dandong Tongda Technology Co., Ltd., Dandong City, China). The soil minerals are listed in Table 2. The mineral composition of saline-alkali soil in the Yellow River Delta is mainly primary minerals, and secondary minerals account for only 6.97% of the total mineral composition.

Table 2 Proportions of minerals of the local saline-alkali soil

Mineral		Percentage/%	
Primary mineral	Quartz	57.63 (0.12)	93.03
	Calcite	8.51 (0.08)	
	Orthoclase	7.05 (0.11)	
	Albite	19.84 (0.16)	
Clay mineral	Illite	5.82 (0.05)	6.97
	Kaolinite	0.18 (0.02)	
	Chlorite	0.97 (0.06)	

Note: Values in parenthesis are standard error.

2.2 Experimental design

Three dredged sediment application layers (surface layer at 0-15 cm, lower layer at 15-30 cm, and plough layer at 0-30 cm) and four dredged sediment incorporation rates (0, 2%, 5% and 10%) were set up in the experiment. There were 10 groups in total, and each group was repeated 3 times. The experimental design is listed in Table 3.

Table 3 Experimental design in the study

Source of variation	Experimental design											
Applying pattern	The upper mixed sediment				The lower mixed sediment				All mixed sediment			
Incorporation rate	0%	2%	5%	10%	0%	2%	5%	10%	0%	2%	5%	10%
Test number	CK	R2	R5	R10	CK	S2	S5	S10	CK	T2	T5	T10
Depth range of sediment incorporation	0-15 cm				15-30 cm				0-30 cm			

The incorporation modes of the dredged Yellow River sediment were as follows. Firstly, a dredged sediment-soil mixture was filled into the 0-15 cm layer, and the saline-alkali soil was filled into the 15-30 cm layer; and this group was set as the upper sediment (R). Secondly, saline-alkali soil was filled into the 0-15 cm layer, and the dredged sediment-soil mixture was filled into the 15-30 cm layer; and this group was set as the lower sediment (S). Finally, a dredged sediment-soil mixture was filled into the 0-30 cm layer, and this group was set as all the sediment (T). According to the proportion of the Yellow River sediment in the dry soil mass, the rates of incorporation were 2%, 5% and 10%, respectively; and the samples not treated with sediment were used as the control group (CK).

An indoor soil column test with one-dimensional constant water head vertical infiltration was carried out, and the test equipment included Markov bottle and soil column. Markov bottle was a transparent glass cylinder with an inner diameter of 10 cm and a height of 50 cm. Small circular holes with a diameter of 1mm are evenly set at the bottom of the soil column, and 1-2 cm of quartz sand is laid at the bottom of the soil column as a filter layer. The soil column was a transparent glass cylinder with an inner diameter of 10 cm and a height of 40 cm. Both the Markov bottle and soil column were calibrated to record water level variations and wetting front depth in the bottle. In order to reduce the effect of the pipe wall on infiltration, it is evenly applied one layer of Vaseline on the inner wall of the soil column before filling the soils. Two layers of permeable and absorbent gauze were laid at the bottom of the soil column to prevent soil particle loss. The filling height of the soil column was 30 cm, divided into 6 layers, each of which was 5 cm high. After mixing the sample evenly, it was subsequently filled it into the soil column and compacted. The layers should be roughened to avoid delamination. After filling, the top of the soil column was covered with a permeable filter paper and a 2-3 cm-thick layer of quartz sand to prevent water erosion.

Before the test started, the height of the Markov bottles was adjusted to keep the water head constant at 4 cm. When the test started, the outlet pipe of the Markov bottle was opened and the changes in the wetting front depth of the soil column and water level height of the Markov bottle were recorded continuously at certain intervals until the end of the experiment. Water supply and time recording ended stopped when the wetting front reached the bottom of the soil column (300 mm).

2.3 Soil microstructure analyses

In this study, the soil microstructure was analyzed only for the soil mixed with Yellow River sediment. Mercury intrusion test and scanning electron microscope were used to analyze the pore characteristics and particle arrangement of soil.

The soil porosity was measured using MIP because the method is relatively straightforward and can be used to obtain reproducible values of pore size distribution. Soil macroporosity (pore size >20 μm) were estimated using MIP. By referring to Liu's pore size division theory[38], the pore sizes of the saline soils in the region were divided into five categories, i.e., ultra-micropore (d < 0.1 μm), micropore (0.1μm ≤ d < 2 μm), small pore (2 μm ≤ d < 10 μm), mesopore (10 μm≤ d <20 μm) and macropore (d ≥20 μm).

To describe the structure of the saline-alkali soils at different sediment incorporation rates, the soil samples were scanned using a JSM-6610LV scanning electron microscope (JEOL, Tokyo, Japan). The overall surface topography of the soil and localized soil areas were observed at low (×200) magnification.

2.4 Infiltration model

The Kostiakov, Philip, and Horton models have been extensively used for the study of movement of water in soil due to their simple description and intuitive physical implications[53]. Therefore, the current study selected these three models to examine the soil infiltration characteristics after amendment was added.

2.4.1 Kostiakov model

The empirical expression of Kostiakov infiltration is:

$$I(t)=mt^n \quad (1)$$

where, $I(t)$ is cumulative infiltration, cm; t is infiltration time, min; m and n are empirical constant parameters, m represents the soil infiltration capacity at the initial stage, and n represents the attenuation rate of the soil infiltration curve.

2.4.2 Philip model

The mathematical expression of Philip infiltration model is:

$$I(t)=St^{0.5}+At \quad (2)$$

where, S is sorptivity, cm/min$^{0.5}$; A is steady infiltration rate, cm/min.

In the Philip infiltration model, the absorption rate S represents the ability of the soil to absorb or release water by capillary force and is an important indicator of the early soil infiltration capacity. The larger the value of S, the greater the infiltration capacity. Stable infiltration rate A is the strength or rate of stable infiltration, which measures the infiltration performance of the soil. As the infiltration time increases, parameter A has a greater influence on the size of the soil infiltration rate.

2.4.3 Horton model

The mathematical expression of the Horton infiltration model is

$$I(t)=at+\frac{1}{b}(b-a)(1-e^{-ct}) \quad (3)$$

where, a is the stable infiltration rate, cm/min; b is the initial infiltration rate, cm/min; c is experience parameter.

3 Results

3.1 Changes in soil wetting front

The application patterns and amount of Yellow River sediment significantly influenced the movement characteristics of soil wetting front. Compared with CK, sediment treatments increased the velocity of the wetting front (p < 0.05, Figure 2). In the upper sediment mixing treatment, the infiltration time was 170 min for CK, 165 min for R2, 156 min for R5, and 150 min for R10 (Figure 2a). Similar trends in infiltration times were observed in the lower mixed sediment and total mixed sediment treatments, with 159 min for S2, 155 min for S5, 129 min for S10, 160 min for T2, 152 min for T5, and 130 min for T10 (Figures 2b and 2c). The

infiltration times for S10 and T10 were significantly lower than that for CK.

The relationship between wetting front and time was further fitted and found to be consistent with the power function: $F=ut^v$, where u and v are empirical constants. The fitting results in Figure 2 shows that the power function can well simulate the wetting front transport law of mixed soil under different Yellow River sediment incorporation rates and application patterns, and the simulated determination coefficient (R^2) for each treatment was greater than 0.995. For the parameter u, R and T application methods showed an increasing trend with the increase of yellow river sediment incorporation rate, while S application method showed a trend of increasing, then decreasing and then increasing. No significant pattern was found in the variation of the power exponent v of the fitted parameters for each treatment, but the parameter v corresponding to the control group was significantly higher than that of the treatment group. This indicated that the application manner and incorporation rates of dredged Yellow River sediment can have a more pronounced effect on the initial water infiltration process that is dominated by the substrate potential.

3.2 Changes in soil cumulative infiltration

The effects of different incorporation rates and application patterns of sediment on cumulative infiltration are shown in Figure 3. From 0 to 100 min, for example, the cumulative infiltration volume increased with the extension of time, and all increases were fast in the beginning and then slow down. In the early stage, due to the low moisture content and strong water absorption capacity, the initial infiltration rate and the slope of the curve were large with an overlapping trend. With the extension of infiltration time, the effects of different sediment treatments on soil water accumulation and infiltration gradually appeared.

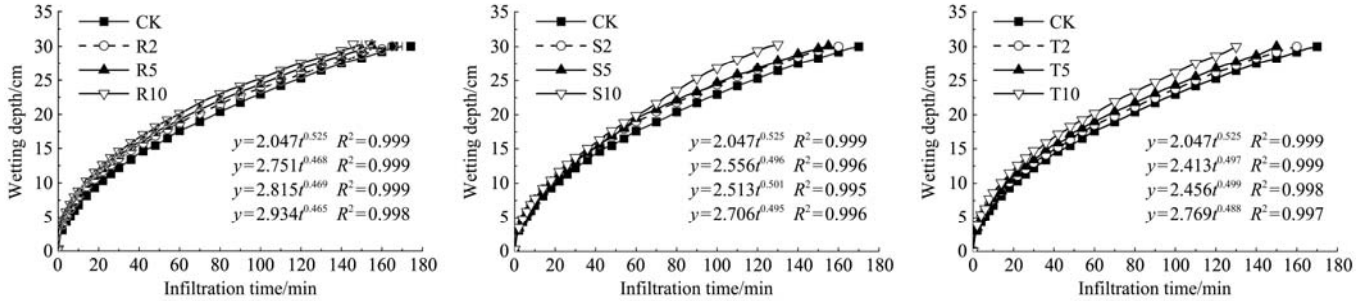

a. Surface layer soil 0-15 cm b. Underlying soil 15-30 cm c. Plough layer soil 0-30 cm

Figure 2 Dynamic changes of the wetting front in the saline-alkali soil amended with sediment at different incorporation rates and different application patterns

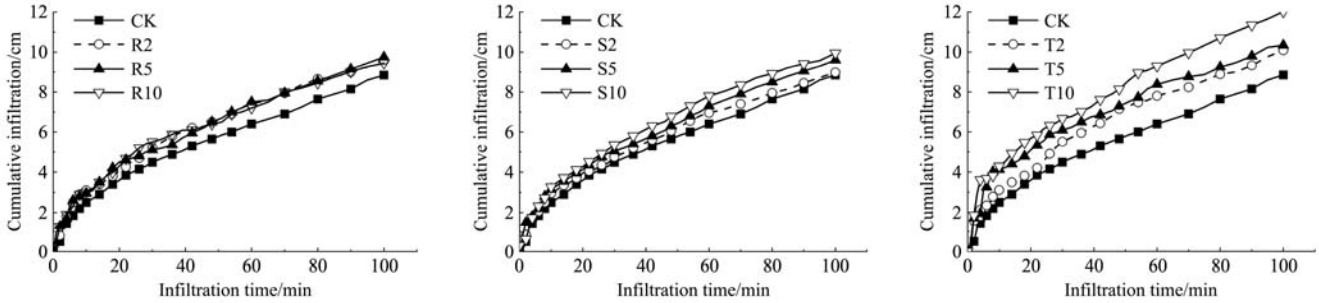

a. Surface layer soil 0-15 cm b. Underlying soil 15-30 cm c. Plough layer soil 0-30 cm

Figure 3 Changes of cumulative infiltration with time under different treatments

At the infiltration time of 100 min, the cumulative infiltration ranged from 88.5 mm (CK) to 110.1 mm (T10) for soils amended with sediment at different incorporation rates and application patterns. For the experimental data, the mean cumulative infiltration generally followed the descending sequence as T10, S10, R5, S5, T5, T2, R10, S2, R2 and CK (Figure 4). Among them, T10 had the largest cumulative infiltration of 110.1 mm, which was 24.41% higher than that of the CK. Statistical analysis revealed that S10, R5, S5, T5 and T2 treatments significantly increased the cumulative infiltration, and their cumulative infiltrations increased by 10.06%, 9.04%, 7.34%, 7.12% and 4.52%, respectively, compared with that of CK. However, the cumulative infiltrations of R2, R10 and S2 treatments were basically the same as that of CK, and the degree of amendment was not significant. This was due to the low soil water content and high soil matrix potential at the beginning of the experiment, soil infiltration was less influenced by the dredged sediment and the curves basically overlapped. With the extension of time, the effect of different Yellow River sediment treatments on the cumulative soil infiltration was gradually revealed.

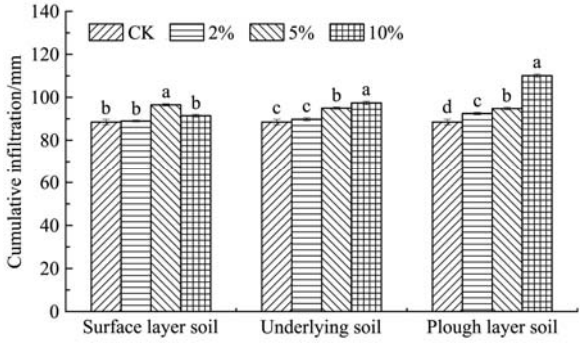

Note: Data recorded at 100 min of infiltration. Different letters above the column indicate significant different at $p<0.05$.

Figure 4 Cumulative infiltration of water into the saline-alkali soil amended with sediment at different incorporation rates and different application patterns

3.3 Fitting parameters of Kostiakov's, Philip's and Horton's infiltration models

The values of parameter m for the three treatments were all higher than that of the CK, with that of the S group being the

smallest and that of the T10 treatment being the largest, which indicated that the initial soil infiltration capacity of the S group was the weakest while that of the T10 was the strongest. The parameter n values of the three treatments had no obvious regularities, whereas the CK had the highest n value, indicating that the sediment treatment reduced the attenuation of soil infiltration and improved the infiltration capacity of soil. The Kostiakov model's fitting results for the soil infiltration process showed that the coefficient of determination R^2 was between 0.992 and 0.999.

Compared with the CK, the soil absorption rates under the other three groups were higher. The absorption rates (Parameter: S in Table 4) of the R and T groups were significantly higher than that of the S group, which indicated that the early sand mixing treatment improved the soil's ability to absorb water through capillary force. Compared with CK, the stable permeabilities (Parameter: A in Table 4) of the three treatments had no significant difference. The fitting results of the Philip infiltration model on the soil infiltration process show that the coefficient of determination R^2 is between 0.991 and 0.998.

The coefficient of determination R^2 for the fit of the Horton infiltration model ranged from 0.991 to 0.998. The parameters including stable infiltration rate (Parameter: a in Table 4) and initial infiltration rate (Parameter: b in Table 4) are basically consistent with the fitting results of the Philip infiltration model, which further showed that the applying dredged sediment improved the infiltration capacity of the soil.

Table 4 Parameters of Kostiakov, Philip and Horton infiltration models

Applying pattern	Sediment incorporation rate/%	Kostiakov			Philip			Horton			
		m	n	R^2	S	A	R^2	a	b	c	R^2
Upper mixed sediment (R group)	0 (CK)	0.64	0.57	0.998	0.73	0.02	0.997	0.05	0.33	0.08	0.996
	2 (R2)	0.95	0.50	0.996	0.96	0.01	0.996	0.05	0.39	0.08	0.991
	5 (R5)	0.86	0.52	0.999	0.90	0.01	0.998	0.06	0.44	0.10	0.993
	10 (R10)	0.78	0.54	0.998	0.84	0.02	0.997	0.06	0.41	0.10	0.998
Lower mixed sediment (S group)	0 (CK)	0.64	0.57	0.998	0.73	0.02	0.997	0.05	0.33	0.08	0.996
	2 (R2)	0.82	0.52	0.997	0.84	0.01	0.997	0.06	0.50	0.15	0.996
	5 (R5)	0.84	0.52	0.997	0.86	0.01	0.998	0.07	0.56	0.17	0.997
	10 (R10)	0.74	0.56	0.995	0.81	0.02	0.993	0.07	0.39	0.10	0.997
All mixed sediment (T group)	0 (CK)	0.64	0.57	0.998	0.73	0.02	0.997	0.05	0.33	0.08	0.996
	2 (R2)	0.86	0.51	0.997	0.88	0.02	0.997	0.05	0.35	0.07	0.996
	5 (R5)	1.20	0.45	0.992	1.08	0.01	0.991	0.05	0.70	0.16	0.995
	10 (R10)	1.28	0.47	0.992	1.18	0.01	0.991	0.07	0.97	0.23	0.993

3.4 Effects of sediment incorporation rates on soil pore size distribution

Compared with CK, Yellow River sediment treatments increased macropores ($p < 0.05$, Figure 5). The mean macro-porosity was 2.31%, 2.90%, 3.52%, and 5.96% for CK, T2, T5, and T10, respectively, with that of T2 being marginally higher than for CK though not statistically significant.

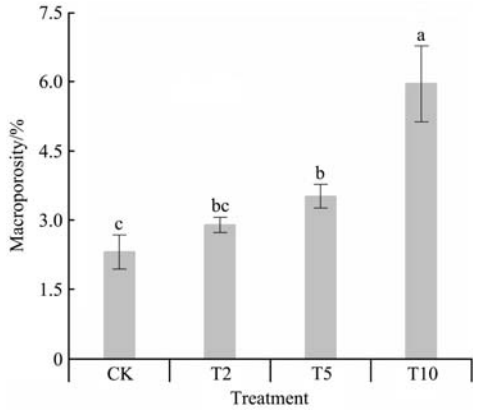

Note: Mean values labeled with the same letter were not significantly different at $\alpha = 0.05$.

Figure 5 Comparison of macroporosity of soil treated with different sediments incorporation rate

The percentages of soil pore group volume under different sediment incorporation rates are listed in Table 5. Similarity, the proportion of macropores to the total soil pores are 5.57%, 5.62%, 6.60%, and 8.23% for CK, T2, T5, and T10, respectively. Additionally, sediment application also significantly decreased the percentage of soil ultra-micro pore (d<0.1 μm) group. This indicated that the applying Yellow River sediment changed both the pore size distribution of soil and the soil porosity.

Table 5 Volume ratios of the pores group in the soil treated with different sediments incorporation rate (%)

Pore diameter /μm	Treatment			
	CK	T2	T5	T10
$d \geq 20$	5.57 (0.07)	5.62 (0.03)	6.60 (0.19)	8.23 (0.02)
$10 \leq d < 20$	55.03 (0.13)	51.87 (0.15)	56.34 (0.09)	56.18 (0.13)
$2 \leq d < 10$	22.47 (0.25)	24.42 (0.01)	19.80 (0.31)	19.36 (0.02)
$0.1 \leq d < 2$	6.82 (0.15)	12.75 (0.07)	10.25 (0.07)	10.46 (0.01)
d<0.1	10.11 (0.17)	5.34 (0.02)	7.01 (0.17)	5.77 (0.15)

Note: Values in parenthesis are standard error.

3.5 Effects of sediment incorporation rate on soil micromorphology

Figure 6 shows the SEM pictures of soil microstructures after treating them with different sediment incorporation rates. As can be seen, the soil particles in the control group were closely arranged without cement connection; and the pores were almost invisible under a low power lens. Dredged sediment application significantly improved the soil pore structure characteristics. In this study, there was no significant difference in the microstructure when the sediment incorporation rate was 2% compared to CK. However, soil microstructure was significantly improved at 5% and 10% dredged sediment incorporation rates.

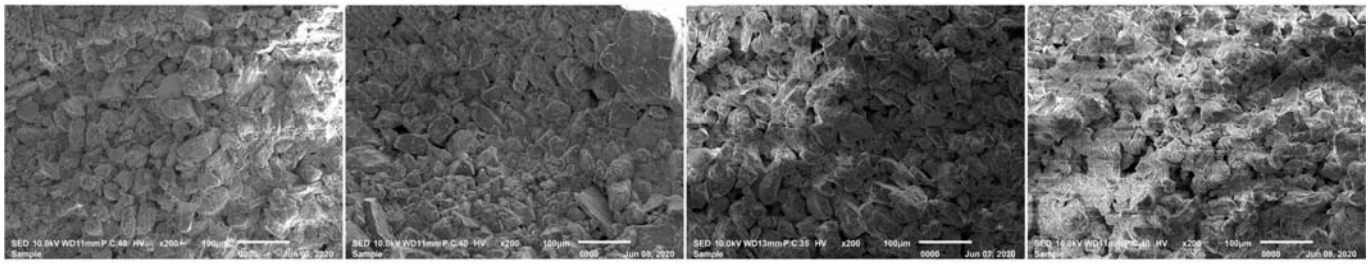

a. 0% sediments incorporation rate b. 2% sediments incorporation rate c. 5% sediments incorporation rate d. 10% sediments incorporation rate

Figure 6 Comparison of microstructure images of soil samples treated with different sediments incorporation rate

4 Discussion

Previous research investigations generally indicate the saline-alkali soils are typically featured with low soil hydraulic conductivity and poor soil structure[39,40]. Similarly, our recent research indicated that the low permeability of soil in the Yellow River Delta is caused by its deteriorated microstructure, which may not be related to its mineral composition[4,35-38]. In line with the conclusion, our experimental data showed that the saturated hydraulic conductivity of saline-alkali soil was 3.58×10^{-5} cm/s (Table 1), and soil infiltration time was 170 min for CK (Figure 2). The existing research generally indicates that mixing sand with the clayed saline soil improved soil texture and infiltration capacity, and with the increase of incorporation rates, the soil infiltration performance increases[41,42]. Similarly, Mao et al.[24,25] reported for the first time that dredged sediment, a poorly graded sand, can significantly improve soil texture, macroporosity, and saturated hydraulic conductivity through field experiments. In our experiments, compared with the control, the infiltration time decreased by about 23.53% for T10 and 24.12% for S10 (Figure 2), and dredged sediment application increased the cumulative infiltration by about 24.41% for T10 and 10.06% for S10 (Figure 3). This result is supported by other studies that have reported that sand additions to saline-alkali soil changed the soil water-salt dynamic movement[43-45].

It is well known that the remediation measures of saline-alkali soil mainly include chemical remediation and physical remediation[21,46,47]. Few studies have considered remedying these soils by improving soil texture conditions[48]. In our experiment, the Yellow River sediment, which is generally regarded as waste by local farmers, was used as an amendment to treat coastal saline-alkali soil. The Chinese government needs to spend a huge amount of funds annually to manage the 1 billion m^3 of sediment deposited in irrigation canals and reservoirs, thus ensuring the effectiveness for water storage and conveyance[25]. Therefore, this research not only helps to save the treatment costs, but also contributes to change the soil texture of the local saline-alkali soil, which is beneficial for environmental protection and agricultural development. This study also indicates that the application of the Yellow River sediment in the underlying layer (15-30 cm) and in the plough layer (0-30 cm) has significant effect on the soil infiltration performance (Figure 2; Table 4). Furthermore, the infiltration effect of the surface layer (0-15 cm) was lower than that of the other two patterns. In clay soils, water and salt have difficulty to infiltrate the soil profile after heavy rainfall or irrigation, and they tend to form surface runoff, which accelerates the loss of soil nutrients and negatively affects plant growth[38,49]. Our findings show that incorporation of dredged sediment into saline soils can change the soil texture and significantly improve its degraded physical properties. Thus, it was suggested to increase soil infiltration by applying Yellow River sediment to the plough layer (0-30 cm) for clay soils.

Amendments such as sand, biochar and gypsum, were incorporated into the soil and improved the soil pore system by forming secondary pores or improving the continuity between pores[50,51]. In this experiment, soil pore size distribution and microstructure were significantly improved with increasing sediment incorporation rate (Figures 5 and 6, Table 5). Compared with the control, dredged sediment application increased the macroporosity by about range from 26% to 158%. Similarly, Qu et al.[52] found that the application of Yellow River sediment on saline soils substantially increased the macro-porosity and hydraulic conductivity. Additionally, soil structure and hydraulic characteristics of saline-sodic soils were also improved with the applications of biochar and frost-heave[31,35,53]. Previous studies generally showed the characteristic parameters, such as porosity, saturated hydraulic conductivity, electrical conductivity and exchangeable sodium percentage, were considered as criteria for saline-alkali soil remediation effectiveness[54-56]. In future studies, soil structure, especially microstructure, should be studied based on one of the criteria for evaluating the effectiveness of soil remediation. This study was limited to indoor soil column experiment, and focused on the effects of dredged sediment incorporation pattern and rates on the infiltration performance and the microstructure of saline-alkali soils, however, its long-term effects on field crop yield and on soil chemical indexes need to be further studied.

5 Conclusions

Soil salinization and sedimentation have long been prominent problems in the Yellow River Delta. In this study, the effects of dredged Yellow River sediment application patterns and incorporation rates on improving water infiltration and microstructure of saline-alkali soils were investigated using indoor soil column experiments. The most typical characteristics of saline-alkali soils are low macroporosity and poor infiltration rate. Results indicated that through dredged sediment treatment, the pore size distribution and microstructure of saline-alkali soils are improved, thus enhancing the soil water infiltration performance. Dredged sediment added to the underlying layer (15-30 cm) and plough layers (0-30 cm) has a higher soil infiltration capacity than the surface layer (0-15 cm). Moreover, the infiltration capacity was improved with the increase of the dredged sediment incorporation rate. Soil macroporosity surveys indicated significantly higher macroporosity values in the treated soil than the control. The Kostiakov model was superior to the Horton and Philip models for estimating soil infiltration in sediment-amended saline-alkali soil. Our findings provide a scientific basis for the application of dredged Yellow River sediments in agricultural production in coastal saline-alkali areas, as well as the selection of

appropriate incorporation rates and application pattern of dredged sediment.

Acknowledgements

This work was supported by the National Natural Science Foundation of China (Grant No. 51574156) and the Key Development Program for Research of Shandong Province (Grant No. 2018GNC110023). The authors would like to thank the anonymous reviews and editors for their constructive suggestions which greatly improve the quality of this manuscript.

[References]

[1] Kahime K, Ben Salem A, El Hidan A, Messouli M, Chakhchar A. Vulnerability and adaptation strategies to climate change on water resources and agriculture in Morocco: focus on Marrakech-Tansifet-Al Haouz region. International Journal of Agriculture and Environmental Research, 2018; 4: 58–77.

[2] Hasini El S, Halima O I, Azzouzi M E, Douaik A, Azim K, Zouahri A. Organic and inorganic remediation of soils affected by salinity in the Sebkha of Sed El Mesjoune-Marrakech (Morocco). Soil & Tillage Research, 2019; 193: 153–160.

[3] Chernousenko G I, Pankova E I, Kalinina N V, Ubugunova V I, Rukhovich D I, Ubugunov V L, Tsyrempilov E G. Salt-affected soils of the Barguzin depression. Eurasian Soil Science, 2017; 50(6): 646–663.

[4] Liu C X, Li K S, Geng Y H, Li Q X. Microscopic structure of soils under different land use types in the Yellow River Delta. Transactions of the CSAE, 2020; 36: 81–87. (in Chinese)

[5] Brinck E, Frost C. Evaluation of amendments used to prevent sodification of irrigated fields. Applied Geochemistry, 2009; 11: 2113–2122.

[6] Ganjegunte G K, Sheng Z, Clark J A. Soil salinity and sodicity appraisal by electromagnetic induction in soils irrigated to grow cotton. Land Degradation & Development, 2014; 25: 228–235.

[7] McFarland M L, Ueckert D N, Hons F M, Hartmann S. Selective-placement burial of drilling fluids: II. Effects on buffalograss and fourwing saltbush. Journal of Environmental Quality, 1992; 21(1): 140–144.

[8] Guo G, Araya K, Jia H, Zhang Z, Ohomiya K, Matsuda J. Improvement of salt-affected soils, Part 1: Interception of capillarity. Biosystems Engineering, 2006; 94: 139–150.

[9] Akudago J A, Nishigaki M, Chegbeleh L P, Alim A. Capillary cut design for soil-groundwater salinity control. Journal of the Faculty of Environmental Science and Technology, 2009; 14(1): 17–22.

[10] Chavez-Garcia E, Siebe C. Rehabilitation of a highly saline-sodic soil using a rubble barrier and organic amendments. Soil & Tillage Research, 2019; 189: 176–188.

[11] Rooney D J, Brown K W, Thomas J C. The effectiveness of capillary barriers to hydraulically isolate salt contaminated soils. Water Air Soil Pollut, 1998; 104: 403–411.

[12] Lee S, Lee S, Bae H, Lee J, Oh Y, Noh T, Lee G. Effect of capillary barrier on soil salinity and corn growth at Saemangeum reclaimed tidal land. Korean Journal of Soil Science and Fertilizer, 2014; 47(6): 398–405.

[13] Strudley M W, Green T R, Ascough I I. Tillage effects on soil hydraulic properties in space and time: State of the science. Soil & Tillage Research, 2008; 99(1): 44–48.

[14] Singh K, Mishra A K, Singh B, Singh R P, Patra D D. Tillage effects on crop yield and physicochemical properties of sodic soils. Land Degradation & Development, 2014; 27(2): 223–230.

[15] Zhao Y G, Wang S J, Li Y, Zhuo Y Q, Liu J. Effects of straw layer and flue gas desulfurization gypsum treatments on soil salinity and sodicity in relation to sunflower yield. Geoderma, 2019; 352: 13–21.

[16] Xie W J, Chen Q F, Wu L F, Yang H J, Xu J K, Zhang Y P. Coastal saline soil aggregate formation and salt distribution are affected by straw and nitrogen application: A 4-year field study. Soil & Tillage Research, 2020; 169: 104535.

[17] Gholizadeh-Sarabi S, Sepaskhah A R. Effect of zeolite and saline water application on saturated hydraulic conductivity and infiltration in different soil textures. Archives of Agronomy and Soil Science, 2013; 59(5): 753–764.

[18] Gharaibeh M A, Eltaif N I, Shra'ah S H. Reclamation of a calcareous saline-sodic soil using phosphoric acid and by-product gypsum. Soil Use and Management, 2010; 26(2): 141–148.

[19] Ahmad S, Ghafoor A, Akhtar M E, Khan M Z. Ionic displacement and reclamation of saline-sodic soils using chemical amendments and crop rotation. Land Degradation & Development, 2013; 24(2): 170–178.

[20] Zhou M, Liu X B, Meng Q F, Zeng X N, Zhang J Z, Li D W, Wang J, Du W L, Ma X F. Additional application of aluminum sulfate with different fertilizers ameliorates saline-sodic soil of Songnen Plain in Northeast China. Journal of Soils and Sediments, 2019; 19(10): 3521–3533.

[21] Yang L, Bian X G, Yang R P, Zhou C L, Tang B P. Assessment of organic amendments for improving coastal saline soil. Land Degradation & Development, 2018; 29(9): 3204–3211.

[22] Sadegh-Zadeh F, Parichehreh M, Jalili B, Bahmanyar M A. Rehabilitation of calcareous saline-sodic soil by means of biochars and acidified biochars. Land Degradation & Development, 2018; 29(10): 3262–3271.

[23] Zhao Y G, Wang S J, Li Y, Liu J, Zhuo Y Q, Chen H X, Wang J, Xu L Z, Sun Z T. Extensive reclamation of saline-sodic soils with flue gas desulfurization gypsum on the Songnen Plain, Northeast China. Geoderma, 2018; 321: 52–60.

[24] Mao W B, Kang S Z, Wan Y S, Sun Y X, Li X H, Wang Y F. Yellow River sediment as a soil amendment for amelioration of saline land in the Yellow River Delta. Land Degradation & Development, 2016; 27: 1595–1602.

[25] Mao W B, Wan Y S, Sun Y X, Zheng Q K, Qv X L. Applying dredged sediment improves soil salinity environment and winter wheat production. Communications in Soil Science and Plant Analysis, 2018; 49: 1787–1794.

[26] Ahmed A. Compressive strength and microstructure of soft clay soil stabilized with recycled bassanite. Applied Clay Science, 2015; 104: 27–35.

[27] Hashemi M A, Massart T J, Salager S, Herrier G, François B. Pore scale characterization of lime-treated sand-bentonite mixtures. Applied Clay Science, 2015; 111: 50–60.

[28] Schluter S, Grossmann C, Diel J, Wu G M, Tischer S, Deubel A, Rucknagel J. Long-term effects of conventional and reduced tillage on soil structure, soil ecological and soil hydraulic properties. Geoderma, 2018; 332: 10–19.

[29] Murmu A L, Jain A, Patel A. Mechanical properties of alkali activated fly ash geopolymer stabilized expansive clay. KSCE Journal of Civil Engineering, 2019; 23: 3875–3888.

[30] Perisic G A, Ovalle C, Barrios A. Compressibility and creep of a diatomaceous soil. Engineering Geology, 2019; 258: 105–145.

[31] Fei Y H, She D L, Gao L, Xin P. Micro-CT assessment on the soil structure and hydraulic characteristics of saline/sodic soils subjected to short-term amendment. Soil & Tillage Research, 2019; 193: 59–70.

[32] Wei Y N, Fan W, Yu B, Deng L S, Wei T T. Characterization and evolution of three-dimensional microstructure of Malan loess. Catena, 2020; 192: 104585.

[33] Wang J D, Li P, Ma Y, Vanapalli S K. Evolution of pore-size distribution of intact loess and remolded loess due to consolidation. Journal of Soils and Sediments, 2018; 19(3): 1226–1238.

[34] Li P, Xie W L, Ronald Y S P, Vanapalli S K. Microstructural evolution of loess soils from the Loess Plateau of China. Catena, 2019; 173: 276–288.

[35] Li K S, Li Q X, Geng Y H, Liu C X. An evaluation of the effects of microstructural characteristics and frost heave on the remediation of saline-alkali soils in the Yellow River Delta, China. Land Degradation & Development, 2021; 32: 1325–1337.

[36] Li K S, Geng Y H, Li Q X, Liu C X. Comprehensive microstructural characterization of saline-alkali soils in the Yellow River Delta, China. Soil Science and Plant Nutrition, 2021; 67(3): 301–311.

[37] Li K S, Geng Y H, Li Q X, Liu C X. Characterization of the Microstructural Properties of Saline-Alkali Soils in the Yellow River Delta, China. Communications in Soil Science and Plant Analysis, 2021; 52(13): 1527–1543.

[38] Liu C X, Li K S, Ma D P. Construction and engineering application of salt-discharging model for local saline-alkali soil with compact structure in the Yellow River Delta. Applied and Environmental Soil Science, 2020; 2020: 1–8.

[39] Zhou R, Li Y Z, Wu J J, Gao M, Wu X Q, Bi X L. Need to link river management with estuarine wetland conservation: A case study in the Yellow River Delta, China. Ocean & Coastal Management, 2017; 146: 43–49.

[40] Xu W S, Li K S, Chen L X, Kong W H, Liu C X. The impacts of

freeze-thaw cycles on saturated hydraulic conductivity and microstructure of saline-alkali soils. Scientific reports, 2021; 11(1): 18655.

[41] Guo T K, Mao W B, Sun Y X, Qu Y J, Wu J L. Amending saline clay soil with fluvial sediments to improve its physical properties and crop productivity. Journal of Irrigation and Drainage, 2021; 40(7): 29–35. (in Chinese)

[42] Zhou L Y, Li R P, Miao Q F, Dou X, Tian F, Yu D D, Sun C Y. Effects of different sand ratios on infiltration and water-salt movement of heavy saline-alkali soil in Hetao irrigation area. Transactions of the CSAE, 2020; 36(10): 116–123. (in Chinese)

[43] Shaygan M, Reading L P, Arnold S, Baumgartl T. Modeling the effect of soil physical amendments on reclamation and revegetation success of a saline-sodic soil in a semi-arid environment. Arid Land Research and Management, 2018; 32(4): 379–406.

[44] Zhang Y H, Gao P L, Zhang Q W, Zhao Y D, Yang D M. Effect of mixing sand with surface soil on moderately salinized soil water-salt transport and summer maize growth. Soil and Fertilizer Sciences in China, 2019; 2: 83–90. (in Chinese)

[45] Li X H, Dang H K, Song N, Shen X J, Gao Y, Sun J S. Effects of biological organic fertilizer and Yellow River sediment mixture on water consumption and growth of winter wheat in saline-alkali land. Transactions of the Chinese Society for Agricultural Machinery, 2020; 51(5): 272–284. (in Chinese)

[46] Drake J A, Cavagnaro T R, Cunningham S C, Jackson W R, Patti A F. Does biochar improve establishment of tree seedlings in saline sodic soils? Land Degradation & Development, 2016; 27(1): 52–59.

[47] Zhao Y G, Wang S J, Li Y, Zhuo Y Q, Liu J. Sustainable effects of gypsum from desulphurization of flue gas on the reclamation of sodic soil after 17 years. European Journal of Soil Science, 2019; 70(5): 1082–1097.

[48] Geng Y H, Liu C X, Li K S, Li Q X. Analysis of relationship between soil structure characteristics and permeability of silty saline-alkali soil in the Yellow River Delta. Water Saving Irrigation, 2020; 2: 27–31+36. (in Chinese)

[49] Li S L, Wang X, Wang S, Zhang Y W, Wang S S, Shangguan Z P. Effects of application patterns and amount of biochar on water infiltration and evaporation. Transactions of the CSAE, 2016; 32(14): 135–144. (in Chinese)

[50] Barzegar A R, Yousefi A, Daryashenas A. The effect of addition of different amounts and types of organic materials on soil physical properties and yield of wheat. Plant and Soil, 2002; 247: 295–301.

[51] Shaygan M, Reading L P, Baumgartl T. Effect of physical amendments on salt leaching characteristics for reclamation. Geoderma, 2017; 292: 96–110.

[52] Qu Y J, Mao W B, Sun Y X, Sun C T, Sun X R. Effects of sand-mixing on saturated water permeability of clay saline soil. Yellow River, 2021; 43(5): 158–162. (in Chinese)

[53] Sun J N, Yang R Y, Li W X, Pan Y H, Zheng M Z, Zhang Z H. Effect of biochar amendment on water infiltration in a coastal saline soil. Journal of Soils and Sediments, 2018; 18(11): 3271–3279.

[54] Luo J Q, Wang L L, Li Q S, Zhang Q K, He B Y, Wang Y, Qin L P, Li S S. Improvement of hard saline-sodic soils using polymeric aluminum ferric sulfate (PAFS). Soil & Tillage Research, 2015; 149: 12–20.

[55] Ahmad S, Ghafoor A, Akhtar M E, Khan M Z. Implication of gypsum rates to optimize hydraulic conductivity for variable-texture saline-sodic soils reclamation. Land Degradation & Development, 2016; 27(3): 550–560.

[56] Xie W J, Wu L F, Zhang Y P, Wu T, Li X P, Ouyang Z. Effects of straw application on coastal saline topsoil salinity and wheat yield trend. Soil & Tillage Research, 2017; 169: 1–6.